Available online at https://asric.africa/engineering-sciences
ASRIC Journal on Engineering Sciences Vol.6(1)(2025) 10-36

Seismic Vulnerability Assessment of Existing Buildings: A case study of Senate Building in Makerere University

Charles Gavamukulya[1], Moses Matovu[1], Allan Ray Okodi[1]

[1]Department of Civil and Environmental Engineering, Makerere University,
gavacharles85@gmail.com mmatovujr@gmail.com, allan.okodi@mak.ac.ug

Corresponding Author: gavacharles85@gmail.com

Received 10 July 2025; revised 22 August 2025; accepted 23 October 2025

Abstract

This study evaluated the seismic vulnerability of existing buildings at Makerere University with focus on Senate Building as a representative structure for mid-rise buildings in the University. Despite Uganda's classification as a low seismic zone, historical earthquakes have exposed significant infrastructure vulnerabilities particularly in educational institutions. The lack of specific locally calibrated models for assessing seismic risk, coupled with the varied and often vulnerable nature of existing construction and limited seismic data in Uganda, makes predicting the seismic vulnerability of existing buildings challenging thereby creating a critical gap in disaster preparedness. The research employed a quantitative methodology combining building inventory classification, structural modeling and fragility curve development. Nonlinear static pushover analysis using SeismoStruct assessed structural capacity and also produced eigenvalue results which enabled identification of ductility limitations. Ground motions from the PEER NGA database were scaled to a target spectrum for Kampala from the GEM framework. Fragility curves were developed using the Capacity Spectrum Method and they quantified the probability of exceeding limit states. Results indicate that Senate building has a total base shear of 4800 kN thereby resisting more lateral force before failure than high rise buildings. However, Senate building reaches the Significant Damage limit state at lower drift values when compared to high rise buildings thereby suggesting brittle behavior. Results also indicate that Senate Building showed moderate resilience reaching the Near Collapse limit state at 0.56g. These findings highlight the urgent need for retrofitting existing buildings in Makerere University particularly for mid-rise buildings and advocate for updating the current seismic code to address seismic vulnerability assessment of existing buildings. This research provides a framework for seismic risk analysis in Ugandan thereby informing retrofitting strategies, policy development, and emergency planning for existing buildings. It bridges a critical gap in regional seismic vulnerability assessments and contributes to global earthquake engineering practices by highlighting the importance of tailored vulnerability evaluations for older building stocks.

Keywords: Seismic Vulnerability, Capacity curves, Fragility Curves

1. Introduction

The occurrence of earthquakes stands as one of the most devastating natural phenomena globally consistently leading to significant human suffering and immense economic and social disruption (Farsangi et al., 2014). In recent decades, a marked increase in losses attributable to natural catastrophes has been observed worldwide (Kassem et al., 2020). This escalation is largely linked to the accelerating growth of the global population, the mushrooming of megacities in areas of high seismic hazard, and the inherent vulnerabilities embedded within modern societies and their technological infrastructure (Calvi et al.,

2006). Catastrophic events such as the 1995 Kobe earthquake which caused an estimated $150 billion in losses, and the 2011 Tohoku earthquake which resulted in a staggering $140 billion in economic damage and over 20,000 fatalities emphasize the financial and human toll that seismic events can exact (Calvi et al., 2006). Therefore, accurately estimating seismic losses is essential for a wide range of stakeholder such as earthquake and geophysical engineers, economic and physical planners, and insurance companies. These estimates play a crucial role in shaping seismic design, supporting disaster mitigation efforts, and enabling efficient emergency management. (Un et al., 2015).

Within the African continent, the East African Rift System (EARS) represents a major active tectonic feature that is characterised by moderate seismicity (Poggi et al., 2016). Despite this classification of moderate activity, historical seismic events within the EARS have demonstrably resulted in considerable damage, primarily due to the intrinsically high vulnerability of local buildings and structures (Tugume & Nyblade, 2009). Uganda which is geographically positioned between the seismically active Western and Eastern branches of the East African Rift System, is thus exposed to varying degrees of seismic hazards (Twesigomwe, 1997). Historical records substantiate this exposure noting several damaging earthquakes including the 1945 Masaka earthquake with 5 fatalities, the 1966 Tooro earthquake with 160 fatalities, and the 1994 Kisomoro earthquake with 8 fatalities (Twesigomwe, 1997). Remarkably, despite these destructive events, the recorded death toll in Uganda has historically been lower than one might anticipate given the prevailing quality of existing buildings. This relative reduction in fatalities is largely attributed to the widespread use of lightweight roofing materials such as grass thatch or galvanized iron sheets particularly on traditional wattle-and-daub or adobe structures (Twesigomwe, 1997). However, the ongoing processes of urbanization and industrial development are progressively extending into areas identified as earthquake-prone within Uganda. This expansion, coupled with the existing structural vulnerabilities, is steadily intensifying the overall seismic vulnerability of the country thereby emphasizing the urgent need for comprehensive seismic hazard and risk evaluation to proactively mitigate future losses (Twesigomwe, 1997).

A key factor contributing to global seismic risk is the prevailing design approach used in many existing buildings (Ferreira et al., 2018). A large share of the built environment, especially older structures, was not specifically engineered to resist seismic forces, resulting in considerable uncertainty about their behavior during earthquakes (Rai, 2008). Most of these buildings were designed mainly to carry gravity loads, with minimal attention given to the lateral forces generated by seismic activity (O'Reilly et al., 2018). This issue is particularly pronounced in Reinforced Concrete (RC) frame buildings constructed before the 1970s, which often followed outdated design standards that existed prior to the introduction of modern seismic codes (Erdil & Ceylan, 2019). This is particularly evident in Reinforced Concrete (RC) frame buildings constructed prior to the 1970s which often adhered to outdated design provisions that predate modern seismic codes (Erdil & Ceylan, 2019). While some older buildings might inherently possess a degree of lateral strength, the acceptable level of damage is subjective and varies with the building's importance, function, and the owner's tolerance for risk (Palacios, 2004). However, without explicit seismic design, the probability of substantial damage or collapse under strong ground motions remains high, positioning older buildings as a primary source of earthquake vulnerability worldwide (Coburn & Spence, 2002).

Compounding the challenge of seismic risk assessment is the human perception of hazard in regions with long recurrence intervals between significant seismic events. A critical factor in limited preparedness is the lack of public awareness regarding the underlying historical seismic risk (Ferreira et al., 2008). Even in areas where high-magnitude earthquakes are infrequent, historical records often reveal a history of devastating events that may be forgotten due to the passage of time without recent major activity. For example, Andalusia in Southern Spain, despite experiencing major earthquakes with intensities of IX or higher in 1504, 1755, and 1884, has traditionally suffered from a lack of awareness due to the long intervals between these events (Ferreira et al., 2008). This pattern illustrates that a prolonged period of seismic latency does not negate the underlying hazard. Such historical seismic patterns, even with extended periods of inactivity, demonstrate that seismic risk is persistent and can manifest unexpectedly, leading to catastrophic consequences if the built environment remains inadequately prepared (Lee et al., 2019). This underscores the vital importance of proactive seismic vulnerability assessment, irrespective of how recent the last major earthquake was.

Current seismic research in Uganda has primarily concentrated on regional seismic hazard assessments rather than detailed building-specific vulnerability evaluations. For instance, Twesigomwe (1997) contributed a probabilistic seismic hazard map of Uganda, drawing upon instrumental data collected between 1900 and 1991. The research calculated mean Peak Ground Acceleration (PGA) values, indicating that most parts of Uganda (excluding direct rift zones) could anticipate PGAs ranging from 0.5 m/s^2 (0.051g) to 0.6 m/s^2 (0.061g) on average once every 50 years. In contrast, areas proximal to the Western Rift were projected to experience PGAs between 1.0 m/s^2 (0.012g) and 2.2 m/s^2 (0.224g) within the same timeframe. According to Twesigomwe (1997), return periods for destructive earthquakes were defined with a PGA of 2.0 m/s^2 (0.204g) revealing that the Western Rift experiences such events with higher frequency averaging. While the research from Twesigomwe (1997) offers invaluable insights into the regional seismic hazard, its primary focus is on the probabilistic assessment of ground motion parameters and not on the detailed, building-specific seismic vulnerability of Uganda's existing building stock. Furthermore, prior seismic hazard studies in Uganda were largely confined to site-specific analyses for hydroelectric projects highlighting a broader gap in comprehensive building vulnerability assessment across the country (Twesigomwe, 1997).

Current seismic codes mainly aim to ensure the safety of newly constructed buildings and their compliance with contemporary design standards. However, a major limitation of these codes is their insufficient attention to evaluating the seismic risk of existing structures (Sarraz, 2015). Because current codes lack clear guidelines for assessing the seismic performance of the existing building stock, it becomes difficult to determine or implement appropriate remedial measures (Rai, 2008). Consequently, there is a pressing need for dependable analytical methods and enhanced seismic retrofitting techniques specifically designed for existing buildings.

As such, this research study was specifically designed to address this critical gap by developing and applying methodologies for seismic vulnerability assessment that are precisely tailored to the unique ground and structural characteristics of existing buildings in Uganda using Makerere University as a case study. The study sought to quantify the seismic vulnerability of the university's buildings by developing fragility curves specific to their building class and structural system. The findings will guide retrofitting, disaster mitigation strategies, and emergency management operations.

2. Methodology

This study addressed the seismic vulnerability assessment of existing buildings in Uganda, given its location within the seismically active East African Rift System (EARS). The research adopted an engineering and probabilistic theoretical perspective to address this question recognizing that seismic vulnerability assessment requires both technical analysis and practical application.

In research design, the choice between quantitative and qualitative paradigms shapes the investigation (Blaxter et al., 1996). As Fellows & Liu (2008) emphasize, these paradigms provide essential frameworks for structuring research to solve specific problems. Quantitative research, as defined by Punch (2005), involves empirical investigation where data is numerical and focuses on measurable phenomena. This approach typically employs statistical methods to analyze relationships between variables (Naoum, 2019). A quantitative paradigm was selected as most appropriate for this study which required measurement of structural responses to seismic forces and probabilistic modeling of damage states.

This study employed analytical modeling as its primary data collection strategy with the Capacity Spectrum Method and Pushover analysis serving as the cores analytical techniques. These methods were chosen over more computationally intensive approaches like the Incremental Dynamic Analysis because it is less computationally intensive and time-consuming. Additionally, it enables direct comparison of structural capacity with seismic demand.

The research followed a systematic implementation of the Capacity Spectrum Method through five stages. Firstly, representative Ugandan building typologies with Makerere University as a case study were classified based on structural characteristics. Secondly, nonlinear pushover analysis developed capacity curves for the midrise typology. Thirdly, appropriate demand spectra were generated considering a target spectrum for Kampala. Fourth, performance points were determined through the intersection of capacity and demand spectra. Finally, fragility curves are developed by statistically analyzing the performance points across multiple intensity levels.

The study concluded by discussing how these Capacity Spectrum Method derived fragility curves can inform seismic risk analysis in Uganda's existing buildings while acknowledging the method's limitations regarding higher-mode effects and complex structural behavior.

2.1 Geographical Area

This research's geographical area of study was limited to Makerere University and is shown in the map in Figure 1.

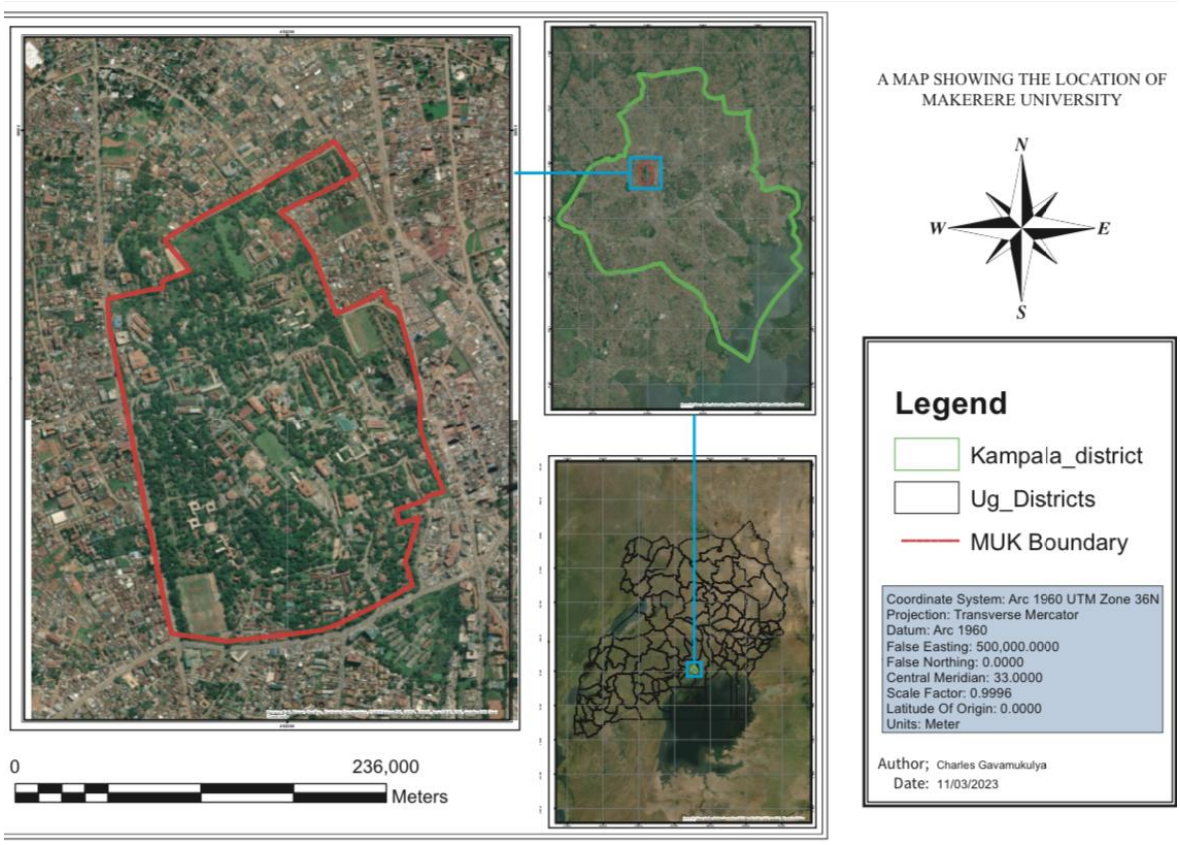

Fig. 1: Map of Makerere University

This study focused on Makerere University, located in Kampala, Uganda, as its primary study area. The university campus presents a living timeline of Ugandan construction practices, featuring colonial-era buildings with distinctive masonry techniques and post-independence reinforced concrete structures, all coexisting within the same geographical area. This diversity provided a valuable opportunity to assess the seismic performance of different building types and construction methods under potential earthquake conditions.

As Uganda's oldest and most prestigious tertiary education institution, it houses invaluable research facilities containing sensitive scientific equipment, historical archives preserving irreplaceable cultural heritage, and specialized laboratories storing hazardous materials, which are all potentially vulnerable to seismic events. The campus's dense daily population of over 20,000 students, faculty, and staff members creates a substantial concentration of human exposure to potential seismic risk. These factors combine to make the university an ideal study area for studying seismic vulnerability where research findings can simultaneously address immediate campus safety concerns while providing insights applicable to similar institutional settings across Uganda.

2.2 Classification of Buildings

In order to classify the existing buildings in Makerere University, a detailed building inventory of the existing buildings in Makerere University was carried out. The classification framework examined seven key parameters for each structure, namely:

i. basic identification, including building name and unique identifier,
ii. typology by primary function (academic, administrative, residential),
iii. precise geospatial location within campus boundaries,
iv. historical context including construction era and period-specific design features,
v. vertical profile documenting the number of stories and basement levels,
vi. structural composition identifying primary load-bearing systems, whether Reinforced Concrete, Steel, or Unreinforced Masonry, and
vii. Documentation status assessing the availability and completeness of architectural/ engineering drawings.

Data collection in the building inventory employed a dual-method approach that consisted of field surveys and a desk study. Field surveys were conducted across the main Makerere University campus to verify locations and the status of buildings across the campus. These on-site investigations were complemented by archival research of Estates and Works Department records, which provided critical historical construction details, original design specifications, and records of subsequent renovations. This document analysis proved particularly valuable for verifying field observations and obtaining structural details not visible during inspections.

Building height, measured by number of storeys, served as the primary classification parameter following the well-established HAZUS classification system (FEMA, 2020). The HAZUS framework was selected for its comprehensive consideration of building height, structural type, and seismic design level, which are factors that have consistently influenced seismic performance (Palacios, 2004). The buildings were divided into three subclasses based on height: low-rise (1–3 floors), mid-rise (4–7 floors), and high-rise (8 or more floors), with each category represented by a typical building (Un et al., 2015). The representative buildings were chosen based on the availability of complete architectural and structural documentation to enable precise modeling and analysis. Other selection factors included their typological representativeness of their subclass, structural system characteristics, and construction era, ensuring they captured the diverse seismic vulnerabilities present across campus.

This paper focuses on Senate building which is the representative structure for mid-rise buildings in Makerere University. This is because Senate Building houses administrative offices, historical records, and serves as a key decision-making center. As such, collapse or severe damage during an earthquake could lead to loss of lives, disruption of university operations, and destruction of valuable assets.

2.3 Structural Modeling

Senate Building was then modeled as a three-dimensional (3D) structural frame using Seismostruct (Sani et al., 2017). Seismostruct is a nonlinear structural analysis software which is widely used for to simulate the seismic response of reinforced concrete structures (Bhatt & Bento, 2014).

The modeling process began with a careful interpretation of the architectural and structural drawings for Senate Building. From these, the typical floor plan, vertical elevation, and sectional profiles were extracted. Special consideration was given to the arrangement of beams and slabs, column spacing, wall positioning, and the overall layout of the lateral load-resisting system. The vertical and horizontal framing systems were replicated to reflect the actual load path and spatial arrangement. Regarding the element sectional properties, including the sizes of columns, beams, and slabs, these were directly obtained from the structural drawings. Each member was assigned cross-sectional dimensions as per the design documents. The reinforcement detailing, including the size, number, and placement of longitudinal bars, stirrups, or ties, was derived from the structural schedules. Where exact detailing was unclear or where ambiguity existed in the provided documents, standardized detailing consistent with typical local engineering practice and code requirements, in this case Eurocode 2, was assumed. A summary of the section details is provided in Table 1.

Table 1: Sectional Properties for Senate Building

Building	Section Properties	Column	Beam
Senate Building	**Depth**	300mm	600mm
	Width	600mm	230mm
	Cover thickness	25mm	25mm
	Longitudinal reinforcement	Φ16	Φ20
	Transverse reinforcement	Φ8 - 150mm c/c	Φ8 - 200mm c/c
	FRP strengthening	No FRP wrapping	No FRP wrapping

The concrete was specified as grade C20/25, and the steel reinforcement was modeled as high-yield deformed bars with a characteristic yield strength (f_y) of 460 MPa, representing the steel strength used in Uganda during the Senate Building's construction. These material properties were incorporated into the Seismostruct model, with the nonlinear behavior of concrete and reinforcing steel simulated using the software's constitutive models, including the Menegotto-Pinto model for steel and the Mander model for both confined and unconfined concrete. The Menegotto-Pinto model is one of the most widely used constitutive models for simulating the cyclic stress-strain behavior of steel in nonlinear analysis software, including Seismostruct. It is a default model in Seismostruct that simulates cyclic loading, captures the Bauschinger effect, and incorporates strain hardening, thereby ensuring compatibility, ease of implementation, and replicability of results. The Mander model is particularly suited for modeling the nonlinear behavior of confined and unconfined concrete in RC structures subjected to seismic loads. It captures confinement effects, provides accurate stress-strain curves, and is one of the most accepted

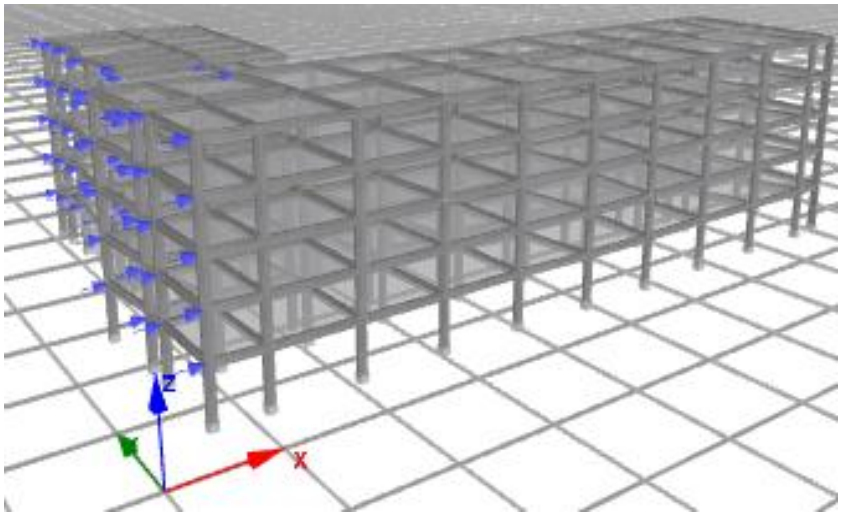

Fig.2: Model for Senate Building

concrete models in seismic analysis literature. Senate building was modeled as a 3D moment-resisting frame with floor diaphragms assumed to act as rigid in-plane. The model for Senate building is shown in the Figure 2.

The vertical load-bearing elements were defined as beam-column elements, and slabs were incorporated using equivalent rigid diaphragms to transmit lateral forces. This reduces the degrees of freedom in the structural model. The building was fixed at the base, assuming fully restrained supports, and soil-structure interaction was not considered in the base model. Plastic hinge length was defined as 16.67% which is a pragmatic simplification in concentrated plasticity models, providing a balance between computational efficiency and capturing of the essential non-linear behavior of reinforced concrete members (Farsangi et al., 2014).

The model was analyzed using both pushover analysis to evaluate its seismic performance. For the pushover analysis, a response control phase loading strategy was adopted, in which specific displacements were applied incrementally and the corresponding base shear was calculated. The target displacement was

determined in accordance with Eurocode 8 Part 3, and three limit states were defined: Damage Limitation (DL), Significant Damage (SD), and Near Collapse (NC). The Damage Limitation state has a 20% probability of exceedance in 50 years, corresponding to a return period of 225 years, and represents a condition where the structure experiences only minor damage while maintaining the strength and stiffness of its elements. The Significant Damage state has a 10% probability of exceedance in 50 years, with a return period of 475 years, reflecting a scenario in which the structure is considerably damaged but retains some residual lateral strength and stiffness. The Near Collapse state, with a 2% probability of exceedance in 50 years and a return period of 2475 years, corresponds to severe structural damage with very low residual lateral strength and stiffness. Using Seismostruct, capacity curves were generated and subsequently converted into Acceleration-Displacement Response Spectra (ADRS) format, which facilitated the development of fragility curves for the building.

Throughout the modeling process, several assumptions were made to address data gaps and to streamline the analytical procedure (Chopra, 2012). All materials were assumed to be homogeneous and isotropic, thereby disregarding any potential variability in material properties due to manufacturing or site conditions (Schnepf et al., 2007). The model did not account for construction defects, aging, or deterioration effects that might influence the structural response over time (Ghosh & Padgett, 2011). Foundation flexibility was also neglected, and the building supports were idealized as fully fixed, eliminating the influence of soil-structure interaction.

Beam-column joints were assumed to behave rigidly, ensuring full moment transfer without joint deformation (O'Reilly et al., 2018). Non-structural elements such as infill walls, staircases, and internal partitions were excluded from the model unless they were considered integral to the structural system or directly contributed to lateral load resistance (Hashmi & Madan, 2008). Additionally, torsional irregularities were not explicitly modeled unless they were apparent from the building geometry. These assumptions allowed for the creation of a simplified yet analytically robust model suitable for the intended seismic performance assessments (Chopra, 2012). The model was calibrated by comparing its fundamental period of vibration with empirical estimates from building code equations, ensuring the dynamic characteristics fell within expected ranges.

2.4 Selection of Ground Motion Data and Intensity Measure

2.4.1 Target Spectrum

The choice of ground motion records was driven by the requirement to align with a target response spectrum representing Kampala's specific seismic hazard. In seismic performance evaluations, such target spectra can be determined using methods that account for the probabilistic characteristics of ground shaking intensity, as highlighted by O'Reilly et al. (2018).

The target spectrum for this study was obtained directly from the Probabilistic Seismic Hazard Analysis (PSHA) results developed by Poggi et al. (2016) within the Global Earthquake Model (GEM) framework. The work by Poggi et al. (2016) provided seismic hazard estimates across Africa, including for four major capitals, among them Kampala in Uganda. In this context, the target ground motion intensity was defined as the 5% damped spectral acceleration (in g), calculated for exceedance probabilities of 10% and 2% in 50 years, corresponding to return periods of approximately 475 and 2475 years, respectively. Due to the significant scarcity of historical earthquake records necessary for accurately calibrating large-magnitude rates, Poggi et al. (2016) avoided using longer return periods or very low probabilities of exceedance. Instead, they applied a set of Ground Motion Prediction Equations (GMPEs) suitable for the tectonic settings of Eastern Africa and computed spectral accelerations at periods of 0.05 s, 0.1 s, 0.2 s, 0.5 s, 1.0 s, and 2.0 s.

The series of hazard maps, produced for different periods corresponding to a 10% probability of exceedance in 50 years, are presented in Figure 3. These maps were used to estimate the spectral acceleration at various periods for Kampala, forming the target spectrum, with periods of (a) 0.05 s, (b) 0.1 s, (c) 0.2 s, (d) 0.5 s, (e) 1.0 s, and (f) 2.0 s. The use of this target spectrum ensured that the selected ground motions adequately reflected the design-level seismic intensity for Kampala and the surrounding areas, thus supporting realistic structural performance and vulnerability assessments.

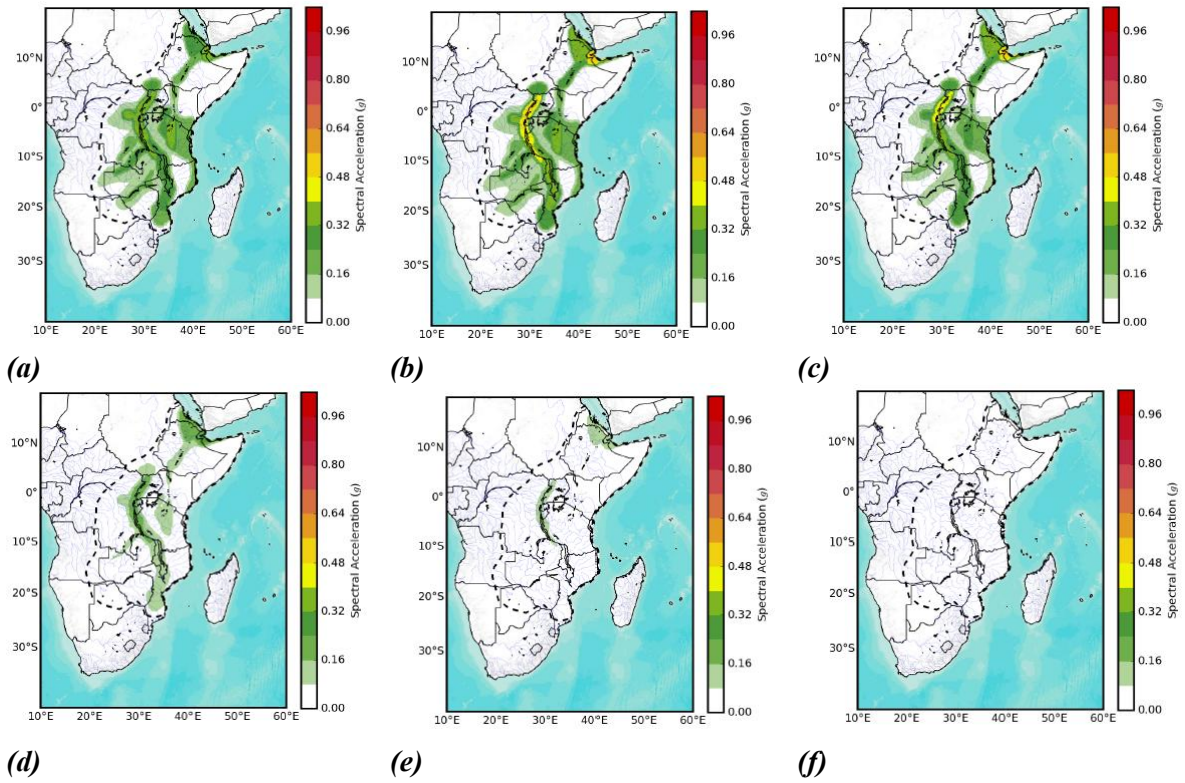

Fig. 31: Seismic Hazard Maps of Spectral acceleration for 10% probability of exceedance in 50 years (Poggi et al. (2016))

2.4.2 Selection of a suite of ground motions

A set of 15 ground motion records was chosen from the PEER NGA database, which is widely recognized as one of the most comprehensive repositories of real earthquake recordings and provides detailed metadata for each record. The PEER NGA database is frequently employed in seismic analyses because it accurately represents the complexities of real seismic events, including duration, frequency content, and spectral characteristics, making it well-suited for realistic evaluation of structural performance under dynamic loading (Banazadeh et al., 2017). While other international databases, such as the European Strong Motion Database, the French Accelerometric Network, and the Swiss Earthquake Database, are also available for selecting ground motions (Nazri, 2018), the PEER NGA database was preferred in this study due to its advanced filtering capabilities and comprehensive documentation.

The selection of ground motions was guided by a set of well-established criteria aimed at ensuring consistency with the seismic hazard characteristics of the study area, as well as compatibility with the dynamic properties of the modeled buildings. A magnitude range of 4.4 to 7.5 was applied to include both moderate and large seismic events, capturing a realistic range of energy release that aligns with potential earthquake scenarios in the East African Rift System (Franchin et al., 2006). Source-to-site distance criteria were specified using both Joyner-Boore distance (R_{JB}) and rupture distance (R_{rup}), with the range set between 10 and 30 kilometers. This distance range was selected to reflect far-to-moderate field conditions and to exclude near-field effects such as velocity pulses that are more prominent in records located less than 10 km from the rupture (Sani et al., 2017).

To reflect local site conditions in Kampala and surrounding areas, which are typically characterized by firm to stiff soils, the shear wave velocity (V_{s30}) was restricted to the range of 360 to 1500 m/s (Cardone et al., 2019). Additionally, a duration filter was applied, with the significant shaking duration (D5–95) set between 15 and 60 seconds to ensure that only records of realistic shaking length were considered. The pulse parameter was left unrestricted to allow inclusion of both pulse-type and non-pulse-type records although most records retrieved under the selected distance criteria were non-pulse type which is consistent with regional tectonics.

The chosen ground motions were scaled to align with the target spectrum previously derived from the Probabilistic Seismic Hazard Analysis (PSHA) by Poggi et al. (2016) from the Global Earthquake Model (GEM) framework. Scaling was performed using the Minimize Mean Squared Error method, which aims to reduce the squared differences between the scaled record spectra and the target spectrum across multiple period points.

A total of 15 ground motions were selected for use in the analysis. While some studies recommend using larger suites for instance 20 to 28 records for Incremental Dynamic Analysis (IDA) and up to 50 or 100 records for probabilistic assessments (Carofilis et al., 2020; Un et al., 2015), the choice of 15 records in this study was driven by both methodological and practical considerations. The main objective was to evaluate median structural response and develop fragility functions rather than perform exhaustive IDA. Literature suggests that for such purposes, suites of 7 to 15 well-scaled records are acceptable, especially when the spectral match is carefully controlled (Nazri, 2018). Furthermore, the use of three-dimensional nonlinear structural models resulted in high computational demands.

2.4.3 Intensity Measure

It is important to note that although multiple parameters exist to quantify ground motion intensity—such as macro seismic scales, peak values like Peak Ground Acceleration (PGA) and Peak Ground Velocity (PGV), and spectral measures including Spectral Acceleration (Sa) and Spectral Displacement (Sd), there is no universal agreement in the literature regarding the most suitable intensity measure for vulnerability assessment (Irfan et al., 2022).

In this study, Spectral Acceleration (Sa) was chosen as the primary intensity measure for developing fragility functions and assessing seismic performance. Sa represents the maximum acceleration experienced by a single-degree-of-freedom (SDOF) oscillator at a specified natural period and damping ratio, making it particularly suitable for evaluating the seismic response of buildings whose dynamic behavior can be approximated by an SDOF system vibrating mainly in its first mode. As highlighted by Yamazaki et al. (2019), Sa offers a more direct correlation between ground motion intensity and structural response, especially when assessed at the building's fundamental vibration period (T_1).

Several studies have highlighted Sa as a preferred intensity measure due to its strong correlation with damage and collapse, particularly for Reinforced Concrete (RC) and moment-resisting frame buildings, which were the focus of this study. Farsangi et al. (2014) note that Sa at the fundamental period (T_1) often provides a better prediction of structural damage than peak measures such as PGA or PGV, as it accounts for dynamic amplification effects that significantly influence a building's inelastic behavior. This makes Sa particularly useful for developing collapse fragility curves, where accurately capturing the initiation and progression of damage is essential (Cardone et al., 2019).

2.5 Development of Fragility Curves

After assembling a suitable set of ground motions and performing nonlinear static pushover analyses on representative buildings, fragility curves were generated using the Capacity Spectrum Method. This approach integrates structural capacity information with seismic demand derived from actual ground motion records, allowing for a performance-based assessment of seismic vulnerability. The core of this method involves representing both the structural capacity and seismic demand in the Acceleration-Displacement Response Spectrum (ADRS) format, enabling a direct comparison between the structure's resistance and the forces imposed by the earthquake.

2.5.1 Conversion of Capacity Curves to ADRS Format

To apply the Capacity Spectrum Method, the capacity curves obtained from the pushover analysis, originally expressed as base shear versus roof displacement, were transformed into equivalent single-degree-of-freedom systems. This transformation utilized modal participation factors and the effective mass derived from the first mode of vibration, which generally governs the seismic response of regular buildings.

The modal participation factor for the representative buildings Uy for Mode 1, the effective modal mass for the modal participation factor U_y, the effective modal mass percentages, the cumulative mass for Uy

at mode 10 were obtained from the eigenvalue analysis which was conducted during the pushover analysis. The total mass of the building was determined using Equation 1.

$$\text{Total Mass} = \frac{Cummulative\ Mass\ at\ Mode\ 10}{Effective\ modal\ mass\ percentage\ at\ Mode\ 10} \qquad \textit{(Equation 1)}$$

The Modal Mass Coefficient (α) was determined using a simplified formula in Equation 2.

$$\alpha = \frac{Effective\ Modal\ Mass\ for\ Uy}{Total\ Mass} \qquad \textit{(Equation 2)}$$

The Base Shear was converted to Spectral Acceleration using the formula in Equation 3.

$$Sa = \frac{V/W}{\alpha}, \qquad \textit{(Equation 3)}$$

where

V = Base Shear

W = Total Weight (Mass * g)

g = 9.81 m/s2

The displacement was converted to spectral displacement using the formula in Equation 4.

$$Sd = \frac{\Delta}{Uy * \phi roof,1}, \qquad \textit{(Equation 4)}$$

where Δ is the displacement, U_y is the participation factor and $\phi_{roof,1}$ is the mode shape.

The assumption that $\phi_{roof,1}=1$ is often valid due to common normalization conventions in modal analysis and simplifies the ADRS conversion and therefore, $\phi_{roof,1}$ was taken to be 1 in all conversions. Therefore, the formula simplifies to Equation 5.

$$Sd = \frac{\Delta}{Uy} \qquad \textit{(Equation 5)}$$

The result was a capacity spectrum in ADRS form plotted as Spectral Acceleration (Sa) against Spectral Displacement (Sd), capturing the inelastic deformation capacity of the structure.

2.5.2 Conversion of the Demand Spectra into ADRS format

The seismic demand was determined using a set of 15 real earthquake ground motion records that had been previously selected and scaled to align with the target spectrum for Kampala, based on the hazard maps by Poggi et al. (2016). Each ground motion was processed to produce a 5%-damped elastic response spectrum, which was subsequently converted into ADRS format. This conversion involved calculating spectral displacement values corresponding to each spectral acceleration using the standard relationship between acceleration, displacement, and period for a single-degree-of-freedom system in the ***Equation 6***.

$$Sd = \frac{T^2}{4\pi^2} * Sa \qquad \textit{(Equation 6)}$$

where Sd is spectral displacement, T is period and Sa is spectra

These ADRS-format spectra represented the expected seismic demand for each ground motion.

2.5.3 Obtaining the Performance Point

With the capacity spectrum and demand spectra expressed in a common format, the next step was to identify the performance point for each ground motion. This point represents the intersection of the structural capacity and seismic demand, indicating the maximum displacement and acceleration the building is expected to experience under that specific ground motion.

Since structures experience inelastic deformation, their damping increases beyond the initial 5% elastic damping, necessitating an iterative procedure. Initially, the elastic demand spectrum was superimposed onto the capacity spectrum to identify an intersection point. This process was repeated for all 15 ground motions, resulting in a set of 15 performance points for each building. These performance points were

then compared to predefined damage state thresholds, which were established based on expected drift limits or spectral displacement values corresponding to slight, moderate, extensive, and complete damage. For each damage state, the number of ground motions exceeding the threshold was recorded, and the corresponding probability of exceedance was determined.

2.5.4 Fragility Curves

These data points were subsequently used to develop fragility curves for each building. A lognormal cumulative distribution function was fitted to the probabilities, with spectral acceleration at the building's fundamental period serving as the intensity measure. In this study, the formulation presented in Equation 7 by Ibrahim and El-Shami (2011) was applied, which is further detailed in Equations 8 and 9.

$$P[D/Sa] = \varphi\left(\frac{In(Sa) - In(\mu)}{\beta}\right), \qquad \textit{(Equation 7)}$$

where P[D/Sa] is the probability of exceeding damage state at spectral acceleration, φ is the standard normal cumulative distribution, μ is the median spectral acceleration corresponding to the damage state, and β is the logarithmic standard deviation, assumed to be 0.4, 0.5 and 0.6 for the respective limit states.

The natural logarithms were computed for a range of Sa values from 1g to 8g. The standardized variable (Z-score) for each damage state threshold was then calculated as in Equation 8.

$$Z = In(Sa) - In(\mu) \qquad (\textit{Equation 8})$$

The cumulative probability of exceeding the damage state at each trial Sa was then determined using the standard normal distribution in Equation 9.

$$P[D/Sa] = \varphi(Z) \qquad (\textit{Equation 9})$$

Similar calculations were carried out for SD, NC, and the Performance Point threshold (PP).

Each fragility curve was defined by a median value (Sa_{50}), representing the spectral acceleration at which there is a 50% probability of exceeding the damage state, and a dispersion parameter (β) representing the variability in response due to record-to-record differences. According to FEMA P-58, β values typically range between 0.3 and 0.6 based on empirical studies, and for this study, a value of 0.4 was used for Damage Limitation, 0.5 for Significant Damage, and 0.6 for Near Collapse.

Although Incremental Dynamic Analysis (IDA) is widely considered the most thorough method for deriving fragility functions, it was not employed in this study due to the complexity of modeling and considerations of time efficiency. IDA involves subjecting each structural model to a series of ground motions that are incrementally scaled to higher intensity levels, often up to 20 steps per record, until structural collapse occurs. While this method offers detailed information on collapse behavior and structural capacity, it requires substantial computational resources and time, particularly when applied to three-dimensional nonlinear models of multiple building types.

In contrast, the Capacity Spectrum Method offers a more efficient alternative, particularly when the goal is to estimate median performance and damage probabilities at representative hazard levels. The use of a realistic suite of scaled ground motions combined with the direct transformation of pushover results into ADRS format allows the method to capture inelastic behavior and ground motion variability without the full complexity of IDA. Moreover, the Capacity Spectrum Method is particularly effective when the seismic demand can be well represented by site-specific response spectra as was the case in this study using hazard-consistent records.

Therefore, the use of the Capacity Spectrum Method in this research was justified by the objective of evaluating the seismic vulnerability of Senate building under realistic hazard conditions while maintaining analytical efficiency. The method provided a reliable and transparent framework for constructing fragility curves that reflect both the capacity of the structure and the probabilistic nature of seismic demand.

4. Findings

The main findings of the study are presented in this section.

4.1 Pushover analysis

The pushover analysis provided results regarding the capacity curve and eigen value analysis for Senate building.

4.1.1 Capacity Curve

The capacity curve, which plots base shear against displacement, illustrates the structural behavior under increasing lateral loads and highlights key performance points such as damage limit states and ultimate capacity of Senate building. Figure 4 shows the capacity curve for Senate building.

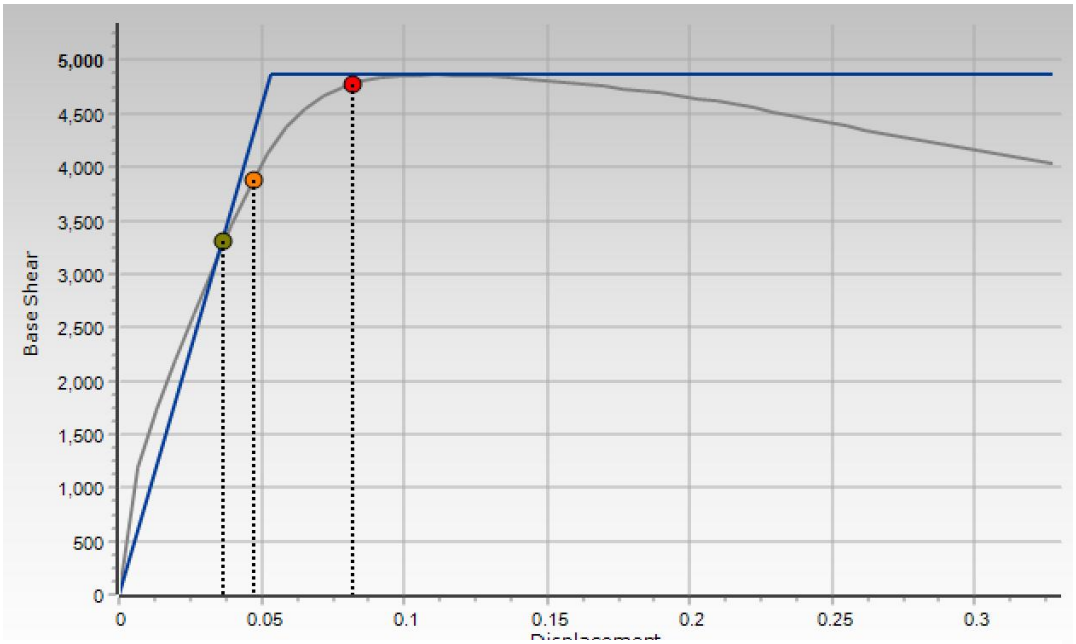

Fig. 4: Capacity curve for Senate Building

There are two key lines on these curves. The grey line represents the actual capacity curve, also known as the pushover curve. It captures the nonlinear response of the structure, beginning with a steep linear segment that reflects the elastic behavior of the structure, where deformation is proportional to the applied load. As the loading increases, the curve transitions into a nonlinear region where the structure begins to yield, indicating the onset of inelastic or plastic behavior. This is followed by a plateau or slight decline in the curve, representing stiffness degradation or strength loss due to accumulated damage in the structural elements.

The blue line is an idealized bilinear representation of the grey capacity curve. This idealization is used to simplify the complex behavior of the actual structure for the purposes of performance-based seismic analysis. The bilinear curve consists of two segments: a linear elastic segment up to the yield point, and a horizontal segment beyond the yield point, which assumes perfectly plastic behavior without strain hardening. This simplification makes it easier to conduct analyses such as the Capacity Spectrum Method, where the nonlinear behavior is approximated for comparison with demand spectra.

The capacity curve for Senate Building in Figure 4 exhibits a steep initial rise in base shear reaching a maximum of 4800 kN at a displacement of approximately 0.045m which is indicative of its fundamental period of 1.82 seconds. The curve plateaus briefly before a gradual decline, suggesting a stable yield plateau followed by a controlled degradation. Damage limit states are marked at 0.037 m for Damage Limitation (DL), 0.047 m for Significant Damage (SD), and 0.077 m for Near Collapse (NC), which reflects the building's progressive deterioration under seismic loading.

4.1.2 Eigenvalue analysis

Modal Periods

An eigenvalue analysis of Senate building provided the natural periods of vibration for the first 10 modes as shown in the Table 2.

Table 2: Modal Periods for Senate Building

Modal Period	Senate Building
1	1.8199
2	1.8199
3	0.8984
4	0.8984
5	0.5779
6	0.5480
7	0.4679
8	0.4679
9	0.3834
10	0.3033

Senate Building displays flexible dynamic profile, with the long fundamental at 1.8199 seconds in both Modes 1 and 2. The modal periods decrease with higher modes, as seen in Mode 3 at 0.8984 seconds and Mode 5 at 0.5779 seconds, capturing progressively faster and more localized vibrational patterns. Senate Building shows clear modal pairings, particularly in the first four modes: Modes 1 and 2 both at 1.8199 seconds, and Modes 3 and 4 both at 0.8984 seconds. This points to symmetry in stiffness and mass distribution in the two principal directions. Senate Building's long periods reinforce its greater flexibility and potentially higher vulnerability to lateral displacements during seismic events.

Effective Modal Mass Percentages

The effective modal mass percentages reveal the significance of each mode in response to earthquake loading in specific directions for Senate building. The effective modal mass percentages for Senate building are shown in Table 3.

Table 3: Effective Modal Mass Percentages for Senate building

Effective Modal Mass Percentages for Senate Building							
Individual Mode							
Mode	**Period**	**U_x**	**U_y**	**U_z**	**R_x**	**R_y**	**R_z**
1	1.8199	0.00%	0.69%	0.00%	0.03%	0.00%	0.08%
2	1.8199	0.00%	0.55%	0.00%	0.03%	0.00%	0.00%
3	0.8984	0.68%	0.00%	0.00%	0.00%	0.02%	0.09%
4	0.8984	0.69%	0.00%	0.00%	0.00%	0.02%	0.11%
5	0.5779	0.001%	6.32%	0.00%	0.23%	0.00%	0.19%
6	0.5480	0.019%	6.17%	0.00%	0.21%	0.00%	3.56%
7	0.4679	0.014%	73.72%	0.00%	2.22%	0.00%	2.00%
8	0.4679	5.07%	0.91%	0.00%	0.02%	0.07%	75.42%
9	0.3834	80.38%	0.03%	0.00%	0.00%	1.26%	5.23%
10	0.3033	0.00%	0.22%	0.00%	0.06%	0.00%	0.02%
Cumulative Mass							
Mode	**Period**	**U_x**	**U_y**	**Uz**	**R_x**	**R_y**	**R_z**
1	1.8199	0.00%	0.69%	0.00%	0.04%	0.00%	0.08%
2	1.8199	0.00%	1.25%	0.00%	0.07%	0.00%	0.08%
3	0.8984	0.69%	1.25%	0.00%	0.07%	0.02%	0.17%
4	0.8984	1.38%	1.25%	0.00%	0.07%	0.03%	0.27%
5	0.5779	1.38%	7.58%	0.00%	0.30%	0.03%	0.47%
6	0.5480	1.40%	13.74%	0.00%	0.51%	0.03%	4.02%
7	0.4679	1.42%	87.46%	0.00%	2.73%	0.03%	6.03%
8	0.4679	6.49%	88.37%	0.00%	2.74%	0.10%	81.45%
9	0.3834	86.87%	88.39%	0.00%	2.74%	1.36%	86.68%
10	0.3033	86.87%	88.61%	0.00%	2.80%	1.36%	86.70%

For Senate building, its transverse (Y-direction) response is primarily governed by mode 7 which alone activates 73.7% of the mass in the Y-direction, while the cumulative participation reaches 88.6% by the 10th mode. For the longitudinal (X-direction) response, a higher mode (Mode 9) dominates with an 80.4% mass activation, reflecting a dynamic response that relies significantly on higher modes, with a cumulative effective mass of 86.9% after 10 modes. The torsional (rotation about the vertical axis) response is similarly influenced by a higher mode (Mode 8), where 75.4% of the mass is activated and by the 10th mode, the cumulative torsional mass is 86.7%. These figures suggest that Senate Building relies on higher modes for its lateral and torsional responses which could be indicative of a more complex or flexible structure.

4.2 Ground motions

4.2.1 Target Response Spectrum

A target spectrum based on seismic hazard maps from GEM Model by Poggi et al. (2016) was generated in the PEER NGA database developed by Ancheta et al. (2014) and used to define the seismic hazard for Makerere University. The spectrum quantifies the expected ground motion accelerations across a range of structural periods and serves as the seismic demand curve for the analysis. The specific spectral acceleration (Sa) values (in units of gravity, g) at corresponding periods (T in seconds) are presented in the ***Fig. 5*** .

Period, T (s)	Spectral Acceleration, Sa (g)
0.00	0.24
0.05	0.32
0.10	0.48
0.20	0.40
0.50	0.24
1.00	0.08

Fig. 5: Target Spectrum output in PEER NGA Database

The spectral acceleration peaks at 0.48g at a short period of 0.1 seconds, indicating a significant demand for structures with high stiffness characteristics. Beyond this peak, the spectral acceleration generally decreases with an increasing period, which is consistent with typical design response spectra. For example, it reduces to 0.24g at 0.5 seconds and further to 0.08g at 1.0 seconds, thereby reflecting lower acceleration demands on more flexible, longer-period structures. This target spectrum provides the fundamental seismic demand for the subsequent structural analyses.

4.2.2 Selection of a Suite of Ground Motions

A set of 15 earthquake ground motion records was obtained from the PEER NGA Database and scaled to match the target spectrum, as illustrated in Figure 6.

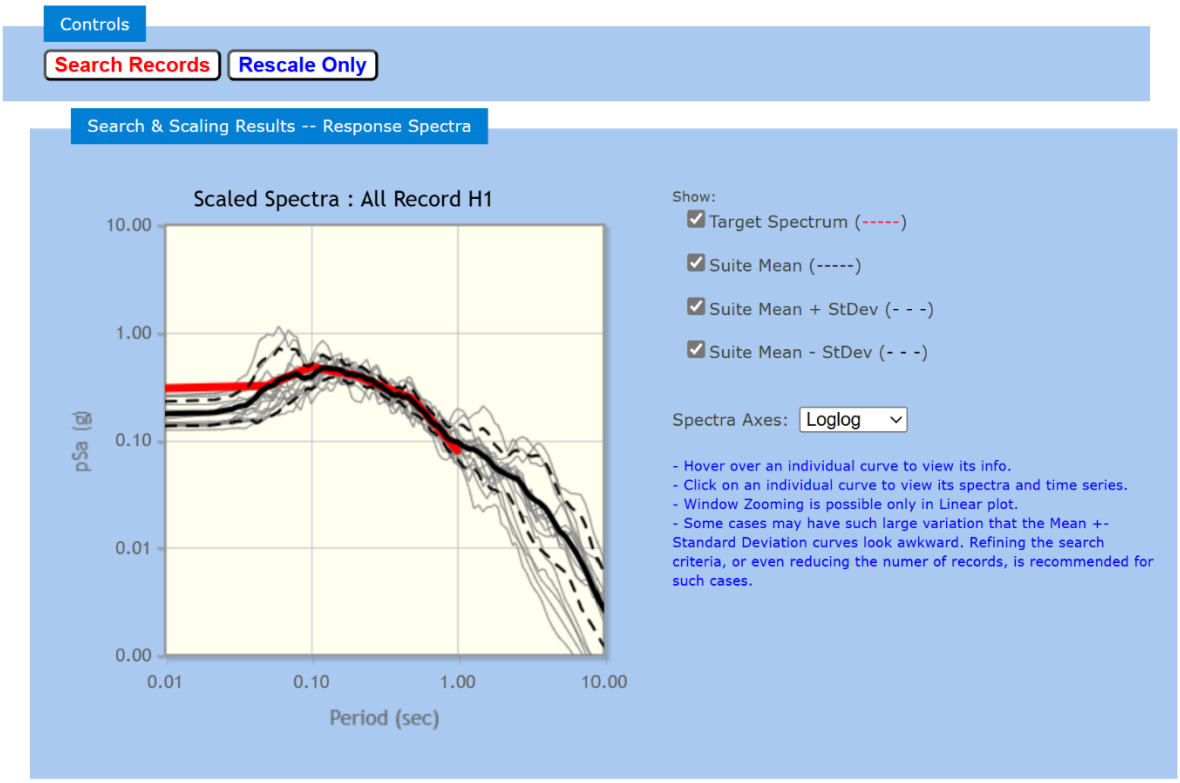

Fig. 6: Suite of ground motions in PEER NGA Database

The suite's mean spectrum demonstrates an excellent and consistent match with the target spectrum across the full range of periods, particularly within the range of engineering interest for the studied buildings, approximately 0.05 to 1.0 seconds. This consistency ensures that, on average, the selected suite accurately represents the site-specific seismic hazard. The plot also clearly shows the inherent variability within the record set, with the Suite Mean ± Standard Deviation (shown by the black dashed lines) encompassing most of the individual scaled records. This spread is vital for capturing the aleatory uncertainty in seismic ground motions and enables a comprehensive assessment of structural response under various plausible earthquake scenarios. The selected ground motions are summarized in the Table 4.

Table 4: Suite of selected 15 ground motions

ID	Earthquake Name	Year	Station Name	Magnitude	Mechanism
TH1	Parkfield	1966	Cholame-Shandon Array	6.19	Strike slip
TH2	Chalfant Valley-01	1986	Benton	5.77	Strike slip
TH3	Chalfant Valley-01	1986	Bishop Paradise Lodge	5.77	Strike slip
TH4	Whitter Narrows-01	1987	Pomona-4th & Locust FF	5.99	Reverse
TH5	Manjil_Iran	1990	Abbar	7.37	Strike slip
TH6	Northridge-06	1994	LA-Temple & Hope	5.28	Reverse
TH7	Chi-Chi_Taiwan-06	1999	TCU076	6.3	Reverse
TH8	Tottori_Japan	2000	OKYH07	6.61	Strike slip
TH9	Cheutsu-oki_Japan	2007	Kawaguchi	6.8	Reverse
TH0	Cheutsu-oki_Japan	2007	Ojiya City	6.8	Reverse
TH11	Cheutsu-oki_Japan	2007	NIG028	6.8	Reverse

ID	Earthquake Name	Year	Station Name	Magnitude	Mechanism
TH12	Cheutsu-oki_Japan	2007	NIGH01	6.8	Reverse
TH13	Iwate_Japan	2008	Tamati Ono	6.9	Reverse
TH14	21530368	2006	Santa Rosa-Hwy 101 & Bicenten	4.5	Strike slip
TH15	21401170	2004	Hog Canyon	4.88	Strike slip

The selected suite encompassed a wide range of seismic characteristics. The records covered a spectrum from moderate events, for example, Magnitude 4.5 for record 21530368, to large earthquakes, for example, Magnitude 7.37 for Manjil_Iran, ensuring a representation of varying energy releases.

A diversity of mechanisms is present, including predominant strike-slip, for example for Parkfield and reverse for Northridge-06, along with reverse oblique for Whittier Narrows-01. Records cover both near-field and far-field conditions, with Joyner-Boore distance (Rjb) ranging from 12.55 km to 28.9 km and rupture distance (R_{rup}) from 12.55 km to 29.65 km.

The selected stations exhibit shear wave velocity, $V_{s,30}$ values from approximately 370 m/s to 940 m/s, accounting for varying local soil stiffnesses. The significant duration (5-95% duration) of the records varies substantially from as short as 15.3 seconds for Northridge-06 to as long as 36.5 seconds for Chuetsu-oki_Japan in the NIGH01 station.

Each record was assigned a specific scale factor ranging from 0.254 for Manjil_Iran to 8.6751 for 21530368 to achieve the desired spectral matching with the target spectrum. The Mean Square Error values for the spectral matching were consistently low, ranging from 0.0333 to 0.0642, indicating a high degree of fidelity in the scaling process and successful alignment with the target spectrum.

4.3 Capacity Spectrum

4.3.1 Conversion of the Capacity Curve to ADRS Format

Data points of base shear and displacement were extracted from the capacity curve in Figure 4 and the conversion to ADRS format using Equations 1 to 5 is presented in Figure 7.

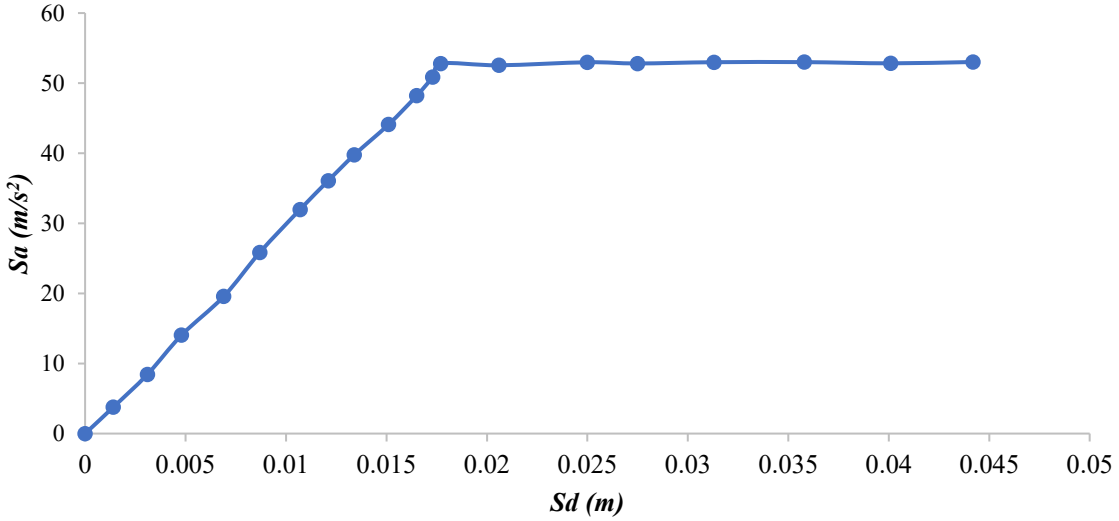

Fig. 72: Capacity curve for Senate building in ADRS format

4.3.2 Conversion of the Demand Spectra to ADRS Format

To overlay the capacity spectrum onto the demand spectrum and determine the performance point, the periods in seconds of the response spectrum were converted into spectral displacements using Equation 6, ensuring that both graphs were represented on the same axes. For instance, the response spectrum of TH1 Parkfield 1966 with a Magnitude of 6.19 from Table 4 above was plotted in the Figure 8.

This response spectrum for TH1 was converted to ADRS format using the formula in Equation 6 and presented in the Figure 9.

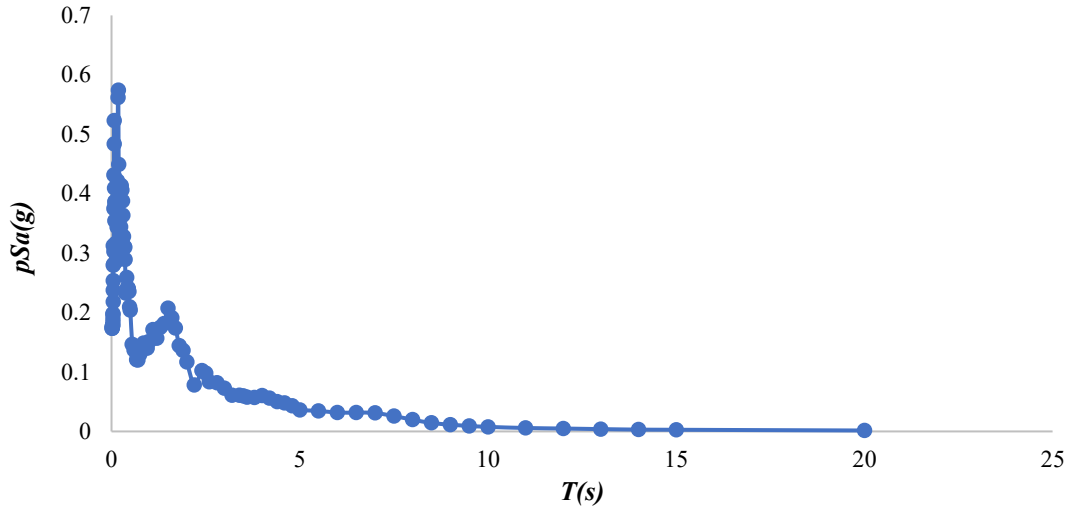

Fig. 8: Demand Spectrum TH1

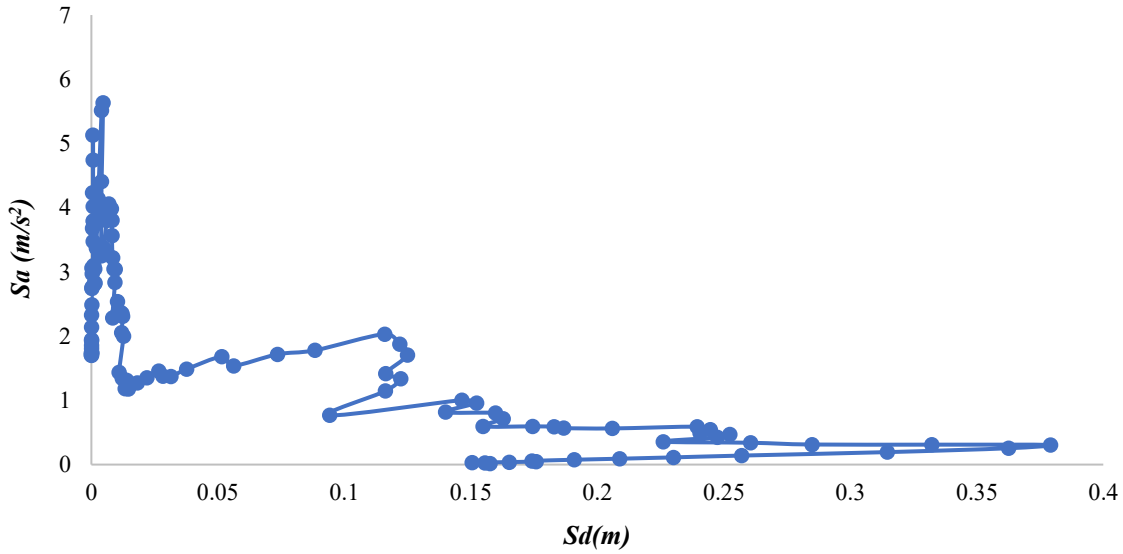

Fig. 9: Demand Spectrum TH1 in ADRS format

4.3.3 Determination of Performance Point

To determine the performance points of the Senate Building, the capacity curve, now expressed in ADRS format as a capacity spectrum, was overlaid onto the demand spectra in ADRS format, as illustrated in Figure 10 for demand spectra TH1. The performance point, representing the intersection of the capacity and demand spectra, indicates the expected displacement and acceleration demands for the specific ground motion. This point reflects the median seismic demand on the building for that particular record.

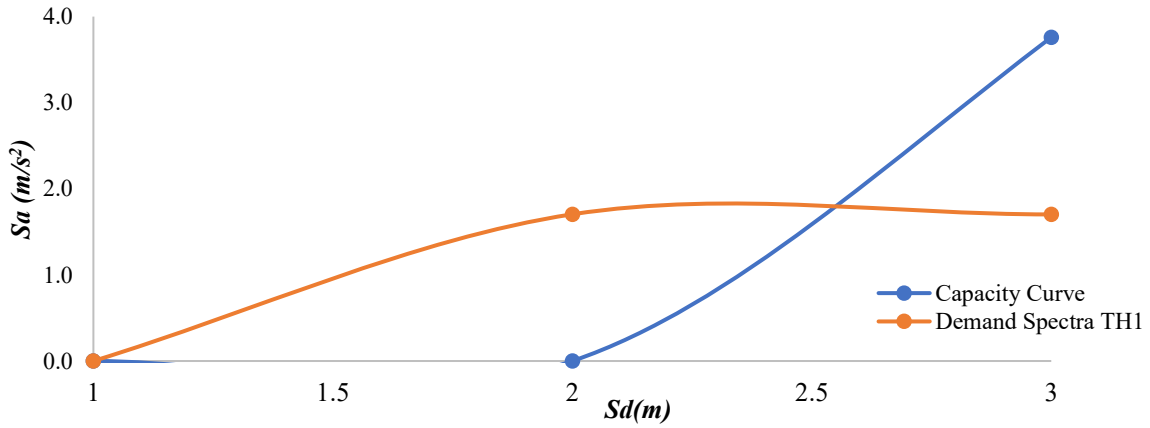

Fig. 30: Performance point for Senate Building with TH1.

The performance points for Senate building using other different spectra are shown in ***Figs. 11 to 12***.

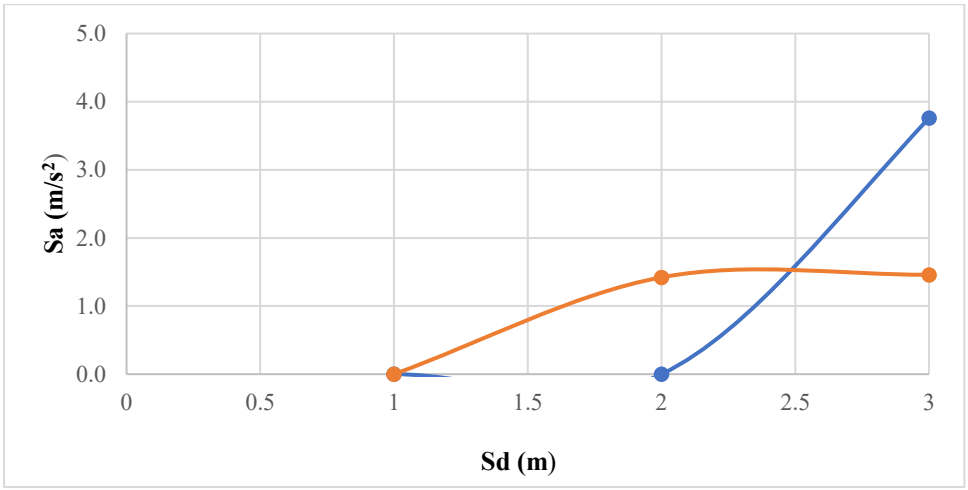

Fig. 11: Performance point for Senate Building with TH2

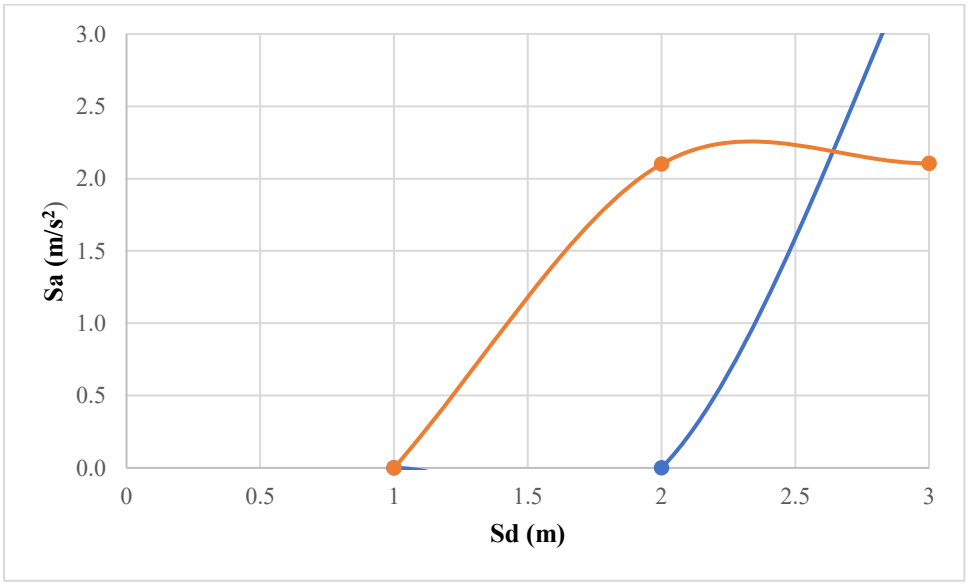

Fig. 12: Performance point of Senate building with TH4

4.4 Development of fragility curves

The fragility curves for the Senate Building were developed using Equations 7 to 9 to quantify the probability of exceeding specified damage states under varying levels of seismic demand.

4.4.1 Definition of Limit State Thresholds

Threshold spectral accelerations (Sa) were established to represent the median capacity of the building to resist each limit state. These values were obtained from the capacity curve of Senate building and presented in Table 5.

Table 5: Limit States for Senate Building

Limit State	Senate Building
Damage Limitation (DL) (Sa)	3.75
Significant Damage (SD) (Sa)	4.43
Near Collapse (NC) (Sa)	5.46

4.4.2 Generation of Fragility Curves

The exceedance probabilities for each damage state, calculated using Equations 7 to 9 across the range of spectral accelerations were then plotted to generate the fragility curves. These curves illustrate the probability of surpassing each damage state (DL, SD, NC) and the Performance Point as a function of Sa for the various demand spectra.

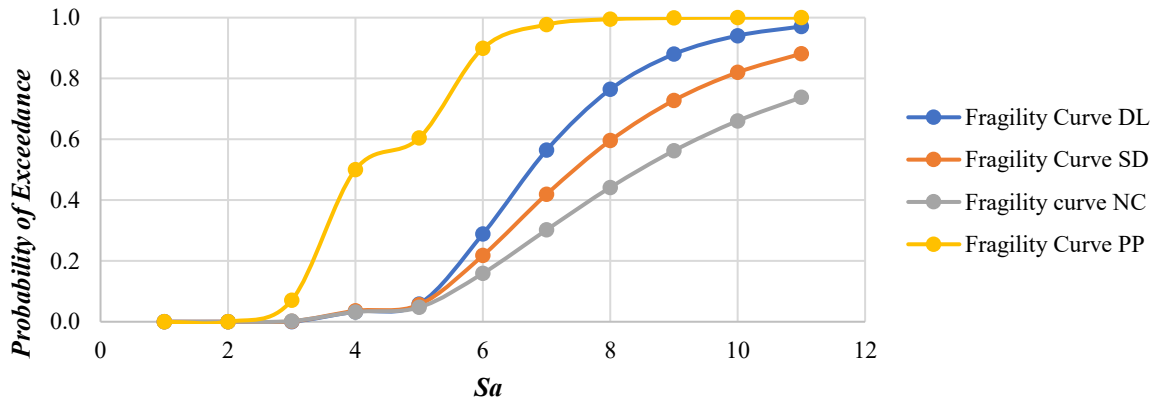

Fig. 13: Fragility curve for Senate Building with TH1

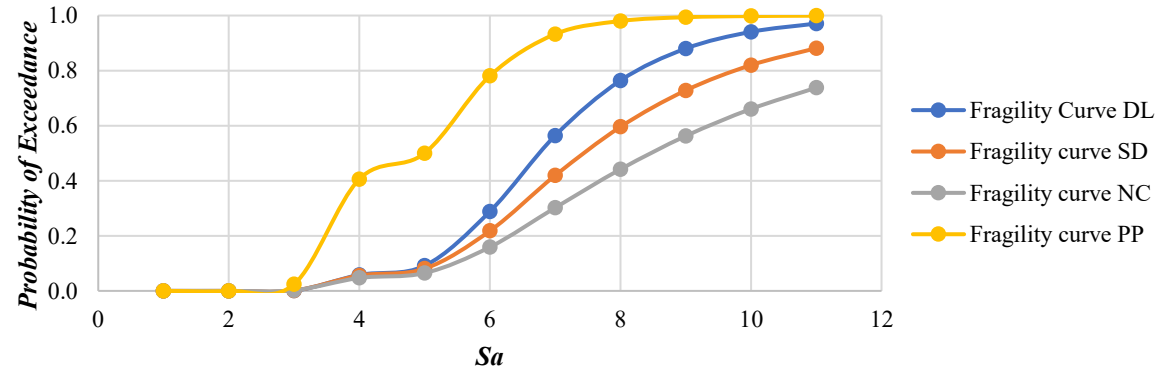

Fig. 14: Fragility Curve for Senate Building with TH4

5. Discussion

A discussion of the results is presented in this section.

5.1 Capacity Curve

The Senate Building's capacity curve shows a gradual initial slope reflecting the moderate stiffness of its Reinforced Concrete frame. The yield point, as shown in Figure 4, occurs at a base shear of 4,800 kN and roof displacement of 0.045 m, followed by a prolonged post-yield plateau with significant ductility (Un et al., 2015). The curve reaches an ultimate displacement of 0.077 m at the NC limit state, indicating substantial energy dissipation capacity before collapse (Hashmi & Madan, 2008). The gradual slope and extended post-yield behavior suggest that the Senate Building can sustain significant deformation without collapse. The Senate Building's RC frame offers greater resistance and ductility, aligning with findings by Un et al. (2015) that Reinforced Concrete frames perform better when engineered. Senate building has a total base shear of 4800 kN thereby resisting more lateral force before failure than high rise buildings.

5.2 Modal periods

The eigenvalue analysis revealed distinct dynamic characteristics for Senate building. Senate Building's long fundamental period of 1.82 seconds indicates greater flexibility, which is typical of mid-rise RC frames (Chopra, 2012). The close pairing of periods in Senate Building's Modes 1 and 2 with both approximately 1.82 seconds, indicates symmetrical stiffness in orthogonal directions thereby reducing torsional vulnerabilities (Sani et al., 2017). Unpaired modes would have suggested potential asymmetry thereby increasing susceptibility to torsional effects as noted by Bhatt and Bento (2014).

The more regular period distribution in Senate Building suggests simpler dynamic responses facilitating more predictable seismic behavior as noted by O'Reilly et al. (2018).

5.3 Effective Modal Mass and Participation Factor

The Senate Building showed significant mass participation in higher modes (Mode 7: 73.7% in Y-direction; Mode 9: 80.4% in X-direction), suggesting that higher modes contribute substantially to its response, which is a characteristic of mid-rise structures (Sani et al., 2017).

Senate Building relied on higher modes with Mode 8 contributing 75.4%, indicating potential torsional vulnerabilities due to irregular mass or stiffness distributions (Bhatt & Bento, 2014). These findings underscore the importance of 3D modeling to capture torsional effects, particularly for taller structures like Senate building (Sani et al., 2017).

5.4 Target Spectrum and Ground motion suite

The target response spectrum and the chosen ground motion records were fundamental elements in the seismic vulnerability assessment carried out at Makerere University. The target spectrum represented the anticipated seismic demand in Kampala, Uganda, reflecting regional hazard characteristics, while the selected ground motions captured the variability of possible earthquake scenarios. These components were essential for assessing the performance of the Senate Building using the Capacity Spectrum Method.

5.4.1 Development of the Target Response Spectrum

The target response spectrum illustrates the expected spectral acceleration (Sa) as a function of period (T) for a specific seismic hazard level, usually expressed by a probability of exceedance, such as 10% in 50 years, corresponding to a 475-year return period. For Kampala, situated in a seismically active area influenced by the East African Rift System (EARS), the target spectrum was developed using Probabilistic Seismic Hazard Analysis (PSHA) studies that account for the local geological and tectonic conditions (Poggi et al., 2016). The spectrum was designed for a reference site class B with 5% damping consistent with Eurocode 8 and ASCE 7-16 standards (CEN, 2004; ASCE, 2016).

The target spectrum for Kampala exhibits a spectral peak of 0.48g at a period of 0.1 seconds, reflecting the dominance of short-period, high-acceleration ground motions typical of shallow crustal earthquakes in the EARS (Poggi et al., 2016). The spectrum decreases to 0.08g at a period of 1.0 seconds and further to 0.03g at 2.0 seconds, indicating lower seismic demands for longer-period structures. This shape is characteristic of regions with frequent moderate-magnitude earthquakes, as observed in the EARS, where faulting occurs at depths of 5–15 km (Midzi et al., 1999). The short-period peak aligns with the dynamic properties of low-rise structures like Livingstone Hall, amplifying their vulnerability, while the reduced

accelerations at longer periods benefit mid-rise and high-rise structures like the Senate Building and Mary Stuart Tower (Karimzadeh et al., 2018).

The target spectrum was derived using a PSHA framework that integrated regional seismicity data, fault models, and Ground Motion Prediction Equations (GMPEs) suitable for the EARS. Due to Uganda's limited seismic monitoring network, the study relied on data from regional studies and international databases (Batte et al., 2014).

5.4.2 Selected Ground Motions

The study employed 15 ground motion records from the PEER NGA-West2 database, chosen to align with the target spectrum and reflect the seismic hazards of Kampala's tectonic setting (Ancheta et al., 2014). The suite included records from both strike-slip and reverse fault events to capture the variety of faulting mechanisms present in the East African Rift System (EARS), compensating for the lack of local strong-motion data (Irfan et al., 2022).

The selection of 15 ground motion records from the PEER NGA database, scaled to align with the target spectrum, ensured consistency with Kampala's seismic hazard. The suite encompassed magnitudes from 4.4 to 7.5 and source-to-site distances between 2.55 km and 29.65 km, capturing a realistic range of seismic scenarios, while the V_{s30} values from 370 m/s to 940 m/s represented local soil conditions (Cardone et al., 2019).

The suite's mean spectrum closely matched the target with low Mean Square Error values from 0.0333 to 0.0642, confirming high reliability in scaling (Banazadeh et al., 2017). The inclusion of diverse fault mechanisms, for instance, strike-slip and reverse mechanisms, and durations from 15.3s to 36.5s ensured comprehensive representation of seismic variability as recommended by Nazri (2018).

The methodology aligns with global standards, such as Eurocode 8 and ASCE 7-16, which emphasize spectral matching and the use of multiple ground motions to capture variability (CEN, 2004; ASCE, 2016). The reliance on the PEER NGA-West2 database is consistent with practices in data-scarce regions, as seen in studies in Ethiopia and Tanzania (Worku & Biggs, 2017). However, advanced seismic regions like California or Japan employ site-specific GMPEs and dense monitoring networks, enabling more precise target spectra and ground motion selection (Abrahamson et al., 2014). Uganda's limited seismic infrastructure (four stations) necessitates greater reliance on international databases, introducing uncertainties that could be mitigated with expanded local monitoring (Batte et al., 2014).

The use of 15 records exceeds the minimum requirements of most codes, enhancing robustness compared to studies using 7–11 records (Cardone et al., 2019). The inclusion of both strike-slip and reverse mechanisms is a strength, as many regional studies focus on a single mechanism, potentially underestimating demand variability (Irfan et al., 2022). However, the absence of normal-fault records, which are also present in the EARS, is a limitation that future studies should address (Poggi et al., 2016).

5.5 Capacity Spectrum Method

The Capacity Spectrum Method (CSM) enabled the combination of structural capacity and seismic demand within the Acceleration-Displacement Response Spectrum (ADRS) framework. The Senate Building's relatively low modal mass coefficient and participation factor suggest a more distributed mass response, reflecting its mid-rise characteristics (Gencturk & Elnashai, 2008). The Senate Building's spectrum indicated higher spectral accelerations up to 0.56g at Near Collapse, suggesting greater resistance (Dya & Oretaa, 2015).

The study's use of the CSM, while less computationally intensive than Incremental Dynamic Analysis, effectively captured median performance and damage probabilities, hence supporting its suitability for regional assessments (Gencturk & Elnashai, 2008). The reliance on the PEER NGA database and Poggi et al. (2016)'s hazard model ensured robust ground motion representation, thereby addressing Uganda's data scarcity challenges (Batte et al., 2014).

5.6 Performance Points and Limit States

5.6.1 Performance Points

The Senate Building exhibits performance points with higher spectral displacements from 0.04m to 0.07 m and spectral accelerations up to 0.5g, reflecting its greater capacity to resist seismic forces. The

building's long fundamental period of 1.82 seconds places it in the lower-acceleration range of the target spectrum with 0.08g at 1.0 seconds thereby reducing its exposure to peak ground accelerations but increasing sensitivity to displacement-driven damage (Farsangi et al., 2014). The performance points indicate that the Senate Building remains below the NC threshold of 0.077 m under most ground motions, suggesting moderate resilience and the ability to sustain significant damage without collapse (Un et al., 2015). This aligns with the building's higher base shear capacity of 4,800 kN and gradual post-yield degradation observed in the capacity curve, indicative of controlled energy dissipation (Hashmi & Madan, 2008). The performance point is at a higher spectral acceleration in comparison to that of high-rise buildings and therefore Senate building is more rigid and likely experiences greater seismic forces. The implications for the Senate Building and similar mid-rise RC structures suggest a need for targeted retrofitting to address these deficiencies, particularly in high-occupancy educational facilities where life safety is paramount.

5.6.2 Limit States

Limit states define the thresholds at which buildings transition to specific damage states, quantified by spectral displacements and linked to qualitative damage descriptions, for example, minor cracks for DL, severe cracking for SD, and structural failure for NC (Ferreira et al., 2018). The limit state thresholds for each building reflect their structural characteristics and dynamic responses, with significant implications for seismic risk mitigation.

The Senate Building's limit states are DL at 0.037 m, SD at 0.047 m, and NC at 0.077 m, showing a wider spread. This wider separation reflects the greater ductility of RC frames, which can absorb more energy before reaching critical failure (Un et al., 2015). The DL threshold indicates that minor damage, such as hairline cracks in infill walls, occurs at similar displacements to low rise buildings, but the higher NC threshold (0.077 m) suggests a greater capacity to withstand seismic demands without collapse (Hashmi & Madan, 2008). The SD threshold associated with repairable damage like spalling concrete indicates that the building can sustain significant damage while maintaining life safety (Yesilyurt et al., 2021). Senate Building's RC frame offers greater ductility with performance points indicating resilience up to 0.5g and limit states showing a wider margin before collapse (Un et al., 2015). Senate Building shows slightly higher displacement demands under reverse mechanisms, which produce stronger spectral accelerations at longer periods (Banazadeh et al., 2017). However, Senate building reaches SD at lower drift than high rise buildings thereby suggesting brittle behavior. The implications include the need for detailed inspections to identify such deficiencies and retrofitting measures such as column jacketing or shear wall additions to enhance ductility and ensure life safety in educational facilities (Cardone et al., 2019).

5.7 Fragility Curves

Fragility curves play a crucial role in assessing the seismic vulnerability of structures by representing the probability of surpassing specific damage states, such as Damage Limitation (DL), Significant Damage (SD), and Near Collapse (NC), as a function of spectral acceleration (Sa). In this study, the fragility curves were developed using the Capacity Spectrum Method, assuming a lognormal distribution of capacity with logarithmic standard deviations (β) of 0.4, 0.5, and 0.6 for DL, SD, and NC, respectively, in accordance with FEMA P-58 guidelines (FEMA, 2020).

5.7.1 Shape and Characteristics of Fragility Curves

The fragility curves for Senate building exhibit unique shapes reflecting their structural typologies, stiffness, ductility, and dynamic properties. The shape of a fragility curve, that is to say, its steepness, position along the Sa axis, and separation between damage states indicate the structure's sensitivity to seismic intensity and its capacity to resist progressive damage (Cardone et al., 2019)

The fragility curves for the Senate Building, a mid-rise reinforced concrete (RC) frame, display a more gradual slope compared to low rise buildings, indicating greater resilience and a wider range of seismic intensities before reaching critical damage states. The DL curve reaches a 50% exceedance probability at approximately 0.25g, SD at 0.35g, and NC at 0.56g. The wider separation between these curves reflects the building's enhanced ductility and capacity to dissipate energy, which is characteristic of RC frames designed with some degree of engineering (Un et al., 2015).

The longer fundamental period of 1.82 seconds places the Senate Building in a lower spectral acceleration range with 0.08g at 1.0 seconds, thereby reducing its exposure to peak ground accelerations but increasing sensitivity to displacement-driven damage (Farsangi et al., 2014). The flatter curves suggest lower variability in response, implying more predictable behavior under seismic loading, which aligns with the building's high modal mass participation in higher modes as shown by 73.7% in Y-direction for Mode 7 and 80.4% in X-direction for Mode 9 and its ability to distribute seismic forces more effectively (Sani et al., 2017).

6. Conclusions

This study conducted a comprehensive seismic vulnerability assessment of existing buildings at Makerere University, focusing on Senate building as a representative structure. The findings provide critical insights into the seismic resilience of the university's building stock and highlight significant vulnerabilities that require urgent attention to enhance disaster preparedness in Uganda's educational infrastructure.

Eigen value analysis showed that Senate building showed a long fundamental period of 1.82s and greater ductility, with a peak base shear of 4800 kN and Near Collapse (NC) at 0.56g suggesting moderate resilience to seismic events. The results showed that high rise buildings like Mary Stuart Hall Tower might have been designed to dissipate energy through larger deformations, while the Senate Building might rely on its strength to resist forces with limited deformation. Eigen value analysis also showed that higher rise buildings like Mary Stuart Hall exhibited higher ductility compared to Senate building. Furthermore, Senate building reached SD at low drift values thereby suggesting brittle behavior by Senate building.

The target response spectrum, derived from Poggi et al. (2016), and the suite of 15 ground motion records from the PEER NGA database accurately represented Kampala's seismic hazard with spectral accelerations peaking at 0.48g for short-period structures. The Capacity Spectrum Method (CSM) effectively integrates structural capacity and seismic demand in the Acceleration-Displacement Response Spectrum (ADRS) format, revealing significant differences in performance.

Fragility curves quantified the probability of exceeding different limit states, confirming Senate Building's moderate resilience with results indicating Near Collapse at 0.56g. These findings align with global studies on older buildings, which highlight the risks posed by outdated design practices and the urgent need for retrofitting, particularly for mid-rise structures.

Overall, the study bridges a critical gap in Uganda's seismic vulnerability assessment by providing a framework for evaluating existing buildings. It emphasizes the inadequacy of current seismic codes, such as US 319:2003, for addressing older structures and highlights the need for enhanced seismic monitoring and data collection to improve hazard assessments in Uganda.

These findings have deep implications for seismic risk management at Makerere University and similar institutions throughout Uganda. The concentration of vulnerable buildings in a densely populated educational environment creates a perfect storm of risk factors: high occupancy levels, critical infrastructure, and structures with limited seismic resistance. The situation is particularly urgent given Uganda's location within the seismically active East African Rift System which has produced damaging earthquakes in recent history, including the 1966 Tooro earthquake that claimed 160 lives. While the university's location in Kampala places it outside the most active rift zones, the historical record shows that significant seismic events can and do occur throughout the country. Based on the findings, the following recommendations are proposed to mitigate seismic risks at Makerere University and inform broader disaster preparedness strategies in Uganda.

For the Senate Building and similar structures, targeted retrofitting such as improving column confinement to enhance ductility would significantly improve seismic performance. Fiber-reinforced polymer (FRP) wrapping of columns and the addition of strategically placed shear walls could provide cost-effective solutions that substantially improve building resilience without requiring complete reconstruction.

The Uganda National Bureau of Standards should revise US 319:2003 to include specific guidelines for assessing and retrofitting existing buildings. These guidelines should incorporate methodologies like the

Capacity Spectrum Method and fragility curve development tailored to local construction practices and seismic hazards.

The current network of few seismic stations in Uganda is inadequate for accurate hazard assessment. Expanding the network, particularly in seismically active regions like the Western Rift, and integrating modern technologies, such as real-time data processing, will improve the precision of ground motion predictions and support site-specific vulnerability assessments.

Future studies should refine fragility curves using region-specific data incorporating local soil conditions, construction quality, and historical seismic records. This will enhance the accuracy of vulnerability assessments and support targeted mitigation strategies for Uganda's built environment.

Educational campaigns should be launched to increase awareness of seismic risks among university stakeholders, including students, staff, and administrators. Training programs for engineers and planners on seismic assessment and retrofitting techniques will build capacity for disaster preparedness.

The study's results should inform university-level disaster management plans, prioritizing evacuation strategies and emergency response protocols for vulnerable buildings. These findings should also guide urban planning and resource allocation for seismic risk reduction across Uganda's educational institutions.

Additional studies should explore the impact of soil-structure interaction, non-structural elements, and aging effects on seismic performance, which were excluded from this study due to data limitations. Incremental Dynamic Analysis could be employed in future research to provide more detailed insights into collapse behavior, despite its computational demands.

7. References

Ancheta, T. D., Darragh, R. B., Stewart, J. P., Seyhan, E., Silva, W. J., Chiou, B. S.-J., Wooddell, K. E., Graves, R. W., Kottke, A. R., Boore, D. M., Kishida, T., & Donahue, J. L. (2014). NGA-West2 Database. Earthquake Spectra, 30(3), 989–1005. doi: 10.1193/070913EQS197M

Anil K. Chopra. (2012). Dynamics Of Structures.

Avşar, Ö. (2009). Fragility Based Seismic Vulnerability Assessment Of Ordinary Highway Bridges In Turkey A Thesis Submitted To The Graduate School Of Natural And Applied Sciences Of Middle East Technical University.

Badal, P., & Motra, G. (2023). Post-2015 earthquake vulnerability of typical RC buildings in Kathmandu Valley. Structures, 57. https://doi.org/10.1016/j.istruc.2023.105111

Banazadeh, M., Gholhaki, M., & Parvini Sani, H. (2017). Cost-benefit analysis of seismic-isolated structures with viscous damper based on loss estimation. Structure and Infrastructure Engineering, 13(8), 1045–1055. https://doi.org/10.1080/15732479.2016.1236131

Batte, A. G., Rümpker, G., Lindenfeld, M., & Schumann, A. (2014). Structurally controlled seismic anisotropy above small earthquakes in crustal rocks beneath the Rwenzori region, Albertine Rift, Uganda. Journal of African Earth Sciences, 100, 579–585. https://doi.org/10.1016/j.jafrearsci.2014.08.001

Bhatt, C., & Bento, R. (2014). The extended adaptive capacity spectrum method for the seismic assessment of plan-asymmetric buildings. Earthquake Spectra, 30(2), 683–703. https://doi.org/10.1193/022112EQS048M

Blaxter, L., Hughes, C., and Tight, M. (2010). How to research. Mainedhead: Open University Press.

Bwambale, B., Bagampadde, U., Gidudu, A., & Martini, F. (2015). Seismic Hazard Analysis for the Albertine Region, Uganda – A Probabilistic Approach. South African Journal of Geology, 118(4), 411–424. https://doi.org/10.2113/gssajg.118.4.411

Calvi, G. M., Pinho, R., Magenes, G., & Bommer, J. (2006). Development of seismic vulnerability assessment methodologies over the past 30 years SERA JRA4 (Risk modelling framework for Europe) ISET Journal of Earthquake Technology. https://www.researchgate.net/publication/241826044

Cardone, D., Perrone, G., & Piesco, V. (2019). Developing collapse fragility curves for base-isolated buildings. Earthquake Engineering and Structural Dynamics, 48(1), 78–102. https://doi.org/10.1002/eqe.3126

Carofilis, W., Perrone, D., O'Reilly, G. J., Monteiro, R., & Filiatrault, A. (2020). Seismic retrofit of existing school buildings in Italy: Performance evaluation and loss estimation. Engineering Structures, 225. https://doi.org/10.1016/j.engstruct.2020.111243

Coburn, A. (Andrew W.), & Spence, R. J. S. (Robin J. S.). (2002). Earthquake protection. J. Wiley.

Doherty, L. (1975). The Seismicity And Tectonics Of Uganda.

Domaneschi, M., Zamani Noori, A., Pietropinto, M. V., & Cimellaro, G. P. (2021). Seismic vulnerability assessment of existing school buildings. Computers and Structures, 248. https://doi.org/10.1016/j.compstruc.2021.106522

Domaneschi, M., Zamani Noori, A., Pietropinto, M. V., & Cimellaro, G. P. (2021). Seismic vulnerability assessment of existing school buildings. Computers and Structures, 248. https://doi.org/10.1016/j.compstruc.2021.106522

Dya, A. F. C., & Oretaa, A. W. C. (2015). Seismic vulnerability assessment of soft story irregular buildings using pushover analysis. Procedia Engineering, 125, 925–932. https://doi.org/10.1016/j.proeng.2015.11.103

El-Kholy, S. A., El-Assaly, M. S., & Maher, M. (2012). Seismic Vulnerability Assessment of Existing Multi-Story Reinforced Concrete Buildings in Egypt. Arabian Journal for Science and Engineering, 37(2), 341–355. https://doi.org/10.1007/s13369-012-0170-0

Erberik, M. A. (2008). Generation of fragility curves for Turkish masonry buildings considering in-plane failure modes. Earthquake Engineering and Structural Dynamics, 37(3), 387–405. https://doi.org/10.1002/eqe.760

Erdil, B., & Ceylan, H. (2019). A Detailed Comparison of Preliminary Seismic Vulnerability Assessment Methods for RC Buildings. Iranian Journal of Science and Technology - Transactions of Civil Engineering, 43(4), 711–725. https://doi.org/10.1007/s40996-019-00234-6

Farsangi, E. N., Rezvani, F. H., Talebi, M., & Hashemi, S. A. H. (2014). Seismic risk analysis of steel-MRFs by means of fragility curves in high seismic zones. Advances in Structural Engineering, 17(9), 1227–1240. https://doi.org/10.1260/1369-4332.17.9.1227

Fellows, R. and Liu, A. (2008). Research Methods for Construction. Oxford: Wiley-Blackwell

Ferreira, T. M., Mendes, N., & Silva, R. (2019). Multiscale seismic vulnerability assessment and retrofit of existing masonry buildings. Buildings, 9(4). https://doi.org/10.3390/buildings9040091

Franchin, P., Pinto, P. E., & Schotanu, M. U. (2006). Seismic loss estimation by efficient simulation. Journal of Earthquake Engineering, 10, 31–44. https://doi.org/10.1080/13632460609350627

Gencturk, B., & Elnashai, A. S. (2008). Development and application of an advanced capacity spectrum method. Engineering Structures, 30(11), 3345–3354. https://doi.org/10.1016/j.engstruct.2008.05.008

Ghosh, J., & Padgett, J. E. (2011). Probabilistic seismic loss assessment of aging bridges using a component-level cost estimation approach. Earthquake Engineering and Structural Dynamics, 40(15), 1743–1761. https://doi.org/10.1002/eqe.1114

Gidaris, I., Padgett, J. E., Barbosa, A. R., Chen, S., Cox, D., Webb, B., & Cerato, A. (2017). Multiple-Hazard Fragility and Restoration Models of Highway Bridges for Regional Risk and Resilience Assessment in the United States: State-of-the-Art Review. Journal of Structural Engineering, 143(3). https://doi.org/10.1061/(asce)st.1943-541x.0001672

Hancilar, U., Çaktö, E., Erdik, M., Franco, G. E., & Deodatis, G. (2014). Earthquake vulnerability of school buildings: Probabilistic structural fragility analyses. Soil Dynamics and Earthquake Engineering, 67, 169–178. https://doi.org/10.1016/j.soildyn.2014.09.005

Hashmi, A. K., & Madan, A. (2008). Current Science Association Damage forecast for masonry infilled reinforced concrete framed buildings subjected to earthquakes in India. Current Science (Vol. 94, Issue 1). https://about.jstor.org/terms

Hazus ®-MH 2.1 Technical Manual. (2003). www.msc.fema.gov

Irfan, Z., Abdullah, & Afifuddin, M. (2022). Development of fragility curve based on incremental dynamic analysis curve using ground motion Aceh earthquake. Web of Conferences, 340. https://doi.org/10.1051/e3sconf/202234002001

Karimzadeh, S., Askan, A., Erberik, M. A., & Yakut, A. (2018). Seismic damage assessment based on regional synthetic ground motion dataset: a case study for Erzincan, Turkey. Natural Hazards, 92(3), 1371–1397. https://doi.org/10.1007/s11069-018-3255-6

Kassem, M. M., & Mohamed Nazri, F. (2022). Integrated approach between seismic resilience and vulnerability indexes with regularity index for vertical irregularity planar frames risk assessment. Bulletin

Kassem, M. M., Mohamed Nazri, F., & Noroozinejad Farsangi, E. (2019). Development of seismic vulnerability index methodology for reinforced concrete buildings based on nonlinear parametric analyses. MethodsX, 6, 199–211. https://doi.org/10.1016/j.mex.2019.01.006

Kassem, M. M., Mohamed Nazri, F., & Noroozinejad Farsangi, E. (2020). The seismic vulnerability assessment methodologies: A state-of-the-art review. Ain Shams Engineering Journal (Vol. 11, Issue 4, pp. 849–864). Ain Shams University. https://doi.org/10.1016/j.asej.2020.04.001

Kassem, M. M., Mohamed Nazri, F., Noroozinejad Farsangi, E., & Tan, C. G. (2021). Comparative seismic RISK assessment of existing RC buildings using seismic vulnerability index approach. Structures, 32, 889–913. https://doi.org/10.1016/j.istruc.2021.03.032

Kaushik, H. B., Rai, D. C., & Jain, S. K. (2006). A case for use of dynamic analysis in designing for earthquake forces. Current Science (Vol. 91, Issue 7). https://www.jstor.org/stable/24094280

Kolekar, S., Vasavada, M., & Patel, V. R. (2016). Development of Fragility Curves for RC Buildings using HAZUS method. International Research Journal of Engineering and Technology. www.irjet.net

Lamprou, A., Jia, G., & Taflanidis, A. A. (2013). Life-cycle seismic loss estimation and global sensitivity analysis based on stochastic ground motion modeling. Engineering Structures, 54, 192–206. https://doi.org/10.1016/j.engstruct.2013.04.001

Lee, S., Panahi, M., Pourghasemi, H. R., Shahabi, H., Alizadeh, M., Shirzadi, A., Khosravi, K., Melesse, A. M., Yekrangnia, M., Rezaie, F., Moeini, H., Pham, B. T., & Bin Ahmad, B. (2019). SEVUCAS: A novel GIS-based machine learning software for seismic vulnerability assessment. Applied Sciences (Switzerland), 9(17). https://doi.org/10.3390/app9173495

Loss, C., Zonta, D., & Piazza, M. (2013). On estimating the seismic displacement capacity of timber portal-frames. Journal of Earthquake Engineering, 17(6), 879–901. https://doi.org/10.1080/13632469.2013.779333

Maasha, N. (1975). The seismicity of the Ruwenzori Region in Uganda. Journal of Geophysical Research, 80(11), 1485–1496. https://doi.org/10.1029/jb080i011p01485

Mander, J. B., Priestley, M. J. N., & Park, R. (1988). Theoretical Stress-Strain Model For Confined Concrete.

Mohamed Nazri, F. (2018). Seismic Fragility Assessment for Buildings due to Earthquake Excitation. Applied Sciences And Technology Computational Mechanics. http://www.springer.com/series/8886

Mohammad, A. F., Khan, R. A., Fatima, E. B., Shaukat, E. A., & Mujtaba, E. M. (2023). Seismic vulnerability assessment of masonry buildings in Karachi. Asian Journal of Civil Engineering, 24(1), 137–151. https://doi.org/10.1007/s42107-022-00493-1

Nafeh, A. M. B., & O'Reilly, G. J. (2023). Simplified pushover-based seismic risk assessment methodology for existing infilled frame structures. Bulletin of Earthquake Engineering, 21(4), 2337–2368. https://doi.org/10.1007/s10518-022-01600-y

Naoum, S. G. (2019). Dissertation research and writing for built environment students. Abingdon, Oxon: Routledge

Nemutlu, Ö. F., Sari, A., & Balun, B. (2023). A Novel Approach to Seismic Vulnerability Assessment of Existing Residential Reinforced Concrete Buildings Stock: A Case Study for Bingöl, Turkey. Iranian Journal of Science and Technology - Transactions of Civil Engineering, 47(6), 3609–3625. https://doi.org/10.1007/s40996-023-01206-7

O'Reilly, G. J., Perrone, D., Fox, M., Monteiro, R., & Filiatrault, A. (2018). Seismic assessment and loss estimation of existing school buildings in Italy. Engineering Structures, 168, 142–162. https://doi.org/10.1016/j.engstruct.2018.04.056

Palacios, S. M. (2004). State Of The Art In Seismic Vulnerability.

Poggi, V., Durrheim, R. J., Mavonga Tuluka, G., Pagani, M., Weatherill, G., Garcia, J., & Nyblade, A. (2016). Global Earthquake Model working together to assess risk A Seismic Hazard Model for Sub-Saharan Africa Technical Report.

Punch, M. (2005). Introduction to Social Research: Quantitative and Qualitative approaches. London: Sage.

Rai, D. C. (2008). A generalized method for seismic evaluation of existing buildings (Vol. 94, Issue 3). www.sefindia .

Riga, E., Karatzetzou, A., Mara, A., & Pitilakis, K. (2017). Studying the uncertainties in the seismic risk assessment at urban scale applying the Capacity Spectrum Method: The case of Thessaloniki. Soil Dynamics and Earthquake Engineering, 92, 9–24. https://doi.org/10.1016/j.soildyn.2016.09.043

Sani, H. P., Gholhaki, M., & Banazadeh, M. (2017). Seismic Performance Assessment of Isolated Low-Rise Steel Structures Based on Loss Estimation. Journal of Performance of Constructed Facilities, 31(4). https://doi.org/10.1061/(asce)cf.1943-5509.0001028

Sarraz, A. (2015). Seismic Vulnerability Assessment of Existing Building Stocks at Chandgaon in Chittagong City, Bangladesh. American Journal of Civil Engineering, 3(1), 1. https://doi.org/10.11648/j.ajce.20150301.11

Schnepf, S., Stempniewski, L., & Lungu, D. (2007). Application Of The Capacity Spectrum Method For Seismic Evaluation Of Structures.

Tarbali, K., & Shakeri, K. (2014). Story shear and torsional moment-based pushover procedure for asymmetric-plan buildings using an adaptive capacity spectrum method. Engineering Structures, 79, 32–44. https://doi.org/10.1016/j.engstruct.2014.08.006

Tugume, F. A., & Nyblade, A. A. (2009). The depth distribution of seismicity at the northern end of the Rwenzori mountains: Implications for heat flow in the Western Branch of the East African Rift System in Uganda. South African Journal of Geology, 112(3–4), 261–276. https://doi.org/10.2113/gssajg.112.3-4.261

Twesigomwe, E. M. (1997). Seismic hazards in Uganda. Journal of African Earth Sciences (Vol. 24, Issue 1).

Un, E. M., Erberik, M. A., & Askan, A. (2015). Performance Assessment of Turkish Residential Buildings for Seismic Damage and Loss Estimation. Journal of Performance of Constructed Facilities, 29(2). https://doi.org/10.1061/(asce)cf.1943-5509.0000547

Vargas-Alzate, Y. F., Lantada, N., González-Drigo, R., & Pujades, L. G. (2020). Seismic risk assessment using stochastic nonlinear models. Sustainability (Switzerland), 12(4). https://doi.org/10.3390/su12041308

Yamazaki, F., Suto, T., Liu, W., Matsuoka, M., Horie, K., Kawabe, K., Torisawa, K., & Inoguchi, M. (n.d.). Development of fragility curves of Japanese buildings based on the 2016 Kumamoto earthquake.

Yesilyurt, A., Zulfikar, A. C., & Tuzun, C. (2021). Seismic vulnerability assessment of precast RC industrial buildings in Turkey. Soil Dynamics and Earthquake Engineering, 141. https://doi.org/10.1016/j.soildyn.2020.106539

Zain, M., Usman, M., Farooq, S. H., & Mehmood, T. (2019). Seismic Vulnerability Assessment of School Buildings in Seismic Zone 4 of Pakistan. Advances in Civil Engineering, 2019. https://doi.org/10.1155/2019/5808256